Performance of a Facility for Measuring Scintillator Non-proportionality

Woon-Seng Choong, *Member, IEEE*, Giulia Hull, William W. Moses, *Fellow, IEEE*, Kai M. Vetter, Stephen A. Payne, Nerine J. Cherepy, and John D. Valentine, *Senior Member, IEEE*

***Abstract*— We have constructed a second-generation Compton coincidence instrument, known as the Scintillator Light Yield Non-proportionality Characterization Instrument (SLYNCI), to characterize the electron response of scintillating materials. While the SLYNCI design includes more and higher efficiency HPGe detectors than the original apparatus (five 25%–30% detectors vs. one 10% detector), the most novel feature is that no collimator is placed in front of the HPGe detectors. Because of these improvements, the SLYNCI data collection rate is over 30 times higher than the original instrument. In this paper, we present a validation study of this instrument, reporting on the hardware implementation, calibration, and performance. We discuss the analysis method and present measurements of the electron response of NaI:Tl from two different samples. We also discuss the systematic errors of the measurement, especially those that are unique to SLYNCI. We find that the apparatus is very stable, but that careful attention must be paid to the energy calibration of the HPGe detectors.**

***Index Terms*—scintillators, electron response, scintillation mechanisms, scintillator non-proportionality, Compton coincidence.**

I. Introduction

We have designed and constructed an instrument to characterize the light-yield non-proportionality of scintillating materials. The instrument is based on the Compton Coincidence Technique (CCT) developed by Valentine and Rooney [1] over 10 years ago. While the original CCT instrument provided an accurate way to measure the electron response in scintillators, the data collection rate was low and it took several weeks to characterize a single scintillator sample. Therefore we have designed and constructed a second-generation high-throughput instrument known as the Scintillator Light-Yield Non-proportionality Characterization Instrument (SLYNCI), which is capable of measuring the electron response of a single scintillator sample in one day with higher statistics and more data points. This considerable reduction in the measurement time dramatically improves the ability of the CCT to test a wide range of scintillator materials and a large number of samples. The high-throughput of SLYNCI will allow us to study the electron responses of many different scintillators in a reasonable time frame. These studies will eventually lead to a deeper understanding of the nature of the light-yield non-proportionality, which is generally accepted as limiting the energy resolution that can be attained with a specific scintillator [2-6]. This paper presents validation studies, the analysis method, and compares the SLYNCI electron response measurement of NaI:Tl with a previous measurement by Rooney and Valentine [7].

Manuscript received June 22, 2007. This work was supported by the U.S. Department of Energy under contracts No. DE-AC02-05CH11231and W-7405-ENG-48.

W.-S. Choong and W. W. Moses are with the Lawrence Berkeley National Laboratory, Berkeley, CA 94720 USA (phone: 510-486-6757; fax: 510-486-4768; e-mail: wschoong@lbl.gov).

G. Hull, K. M. Vetter, S. A. Payne, N. J. Cherepy, and J. D. Valentine are with the Lawrence Livermore National Laboratory, Livermore, CA 94551 USA.

II. SLYNCI

The design of the SLYNCI is described in detail in [8]. The instrument employs five high-purity germanium (HPGe) detectors, each located at a different scattering angle 10 cm away from the scintillator sample under study and measures the energy of the scattered gamma ray. The array of 21%–34% HPGe detectors significantly reduces the data collection time because data can be collected at multiple electron energies simultaneously. A collimated 1 mCi Cs-137 source illuminates the scintillator sample from a distance of 18 cm. The scintillator is coupled to a Hamamatsu photomultiplier tube (PMT) model R6231. The scattered electron is absorbed in the scintillator and the scattered gamma ray is detected in an HPGe detector. Each HPGe detector (about 5 cm in diameter) subtends about 30° and thus observes Compton scattered gamma rays with a relatively broad range of energies. The electron energy deposited in the scintillator for each event can be calculated by subtracting the scattered gamma ray energy measured in the HPGe detector from the incident source energy (661.657 keV). The energy resolution of each HPGe detector is 1–2 keV.

The instrument is designed to sample the scattered electron energy deposited in the scintillator that is between 1 and 466 keV. Historically, this energy range has proven sufficient to characterize electron response for all scintillators. The electron response below 20 keV is especially critical in studying scintillation mechanisms. In order to cover the entire range of scattering angles, the source and collimator are placed on a rotating stage so that the angle of the gamma ray incidence on the scintillator sample can be rotated by 15°. A computer-controlled pneumatic system is used to rotate the source-collimator assembly between the two positions (0° and

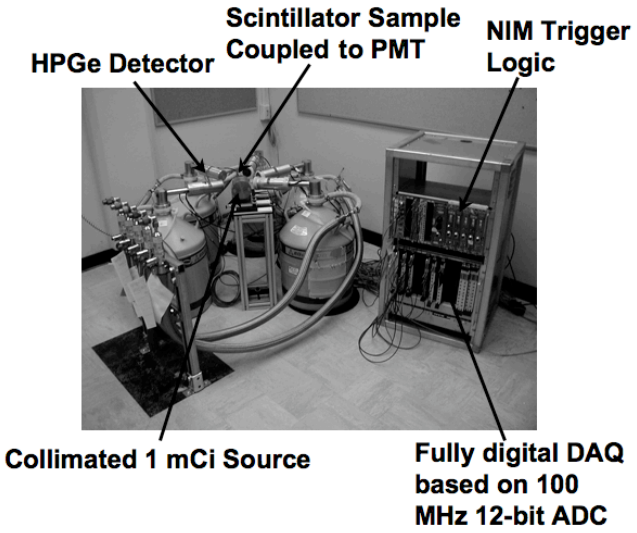

Fig. 1. Photograph of the SLYNCI

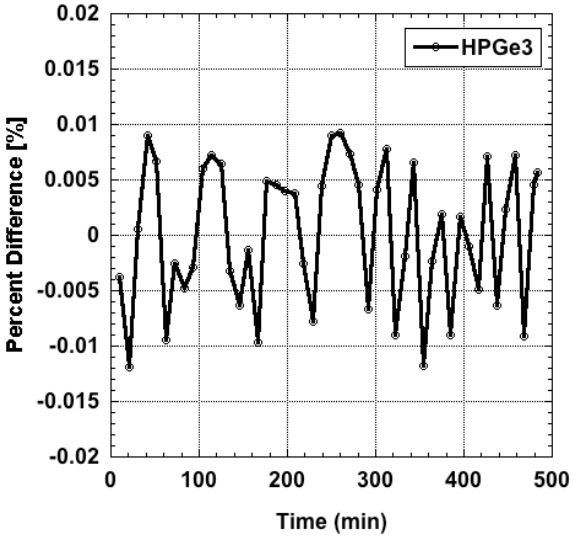

Fig. 2. Variation of the photopeak positions of one of the HPGe detectors (HPGe3) over a period of 8 hours (the typical data acquisition time of an experimental run). Similar variations in the photopeak positions are observed in the other HPGe detectors.

15°). Data are collected at both source-collimator positions. Fig.1 shows a photograph of the SLYNCI.

A fully digital data acquisition system is implemented to read out the PMT and HPGe detectors. The DAQ system utilizes two digitizer 6U VME boards from Struck Innovative System (SIS), one for the PMT and another for the HPGe detectors as shown in Fig. 1. Each digitizer board consists of eight channels of analog-to-digital converters (ADCs) with sampling rate of 100 MHz and 12-bit resolution. In addition, each board has an onboard FPGA, which increases the overall flexibility of the DAQ system, and in particular, provides a digital signal to trigger the electronics whenever any of the detectors serviced by that board observes a pulse that is above a pre-determined amplitude. A separate FPGA-based trigger system monitors the signals from the two ADC boards and initiates readout of the ADCs whenever the trigger conditions are met. Each time readout is initiated, a 40 μs long record (4000 consecutive ADC samples spaced 10 ns apart) from each detector channel that is above threshold is transferred from the VME crate to the host computer. The energy is determined by applying a trapezoidal filter to each record.

III. SLYNCI Performance and Data Analysis

A. Data Collection

The SLYNCI system is triggered by one of two event topologies: coincidence events or singles events. Coincidence events are defined as events with a signal in the PMT in time coincidence with a signal with any of the five HPGe detectors within a coincidence window of about 1000 ns (this window is adjustable from 25 ns to 1 μs in 25 ns steps.) Singles events are those with energy deposited in exactly one detector (either the PMT or any of the HPGe detectors) and are used for calibrating and monitoring the detectors. These occur relatively frequently, either because of photoelectric interaction in the scintillator (which create PMT singles) or because of events where the gamma ray misses the scintillator and interacts in a HPGe detector (which create HPGe singles). These singles events are interspersed with coincidence events during data acquisition, and are usually pre-scaled to a rate of ~100 cps, whereas the coincidence event rate is typically 50 cps. For the measurement of the non-proportionality of a scintillator sample, data are collected for about 8 hours for each of the two source-collimator positions.

For calibration, a Cs-137 source is used to excite the scintillator and HPGe detectors. Singles events are collected and the pulse height spectrum for each detector is histogrammed. The 662 keV photopeak positions are determined by fitting the peaks with a Gaussian function. A series of 10 minute run are collected over a period of a few hours, and within each run the photopeak positions of the HPGe and the PMT can be measured to a statistical accuracy of 0.001% and 0.02% respectively.

B. HPGe Stability

Because the measurement of the energy deposited in the scintillator with SLYNCI relies solely on the measurement of the scattered gamma ray energy in the HPGe detector (as opposed to the first generation instrument, which depended on the position of the shielding), accurate energy calibration for the HPGe detectors is critical. It is especially critical for the HPGe placed on the opposite side of the scintillator from the source (sampling the low electron energy deposited in the scintillator) because the electron response measurement is very sensitive to the incorrect calibration of this detector, as discussed in Section IV. Fig. 2 shows the variation of the photopeak positions of one of the HPGe detectors (the one placed on the opposite side to the source or HPGe3) over an eight hour period. The statistical error for each data point is ~0.001%. The maximum variation in the photopeak positions is about 0.01%, and the time scale of these fluctuations is significantly shorter than the data collection time. Similar variations in photopeak positions are observed in the other HPGe detectors. However, these variations can be removed by calibration. The singles events are interspersed with the coincidence events, and the singles events are used to create a

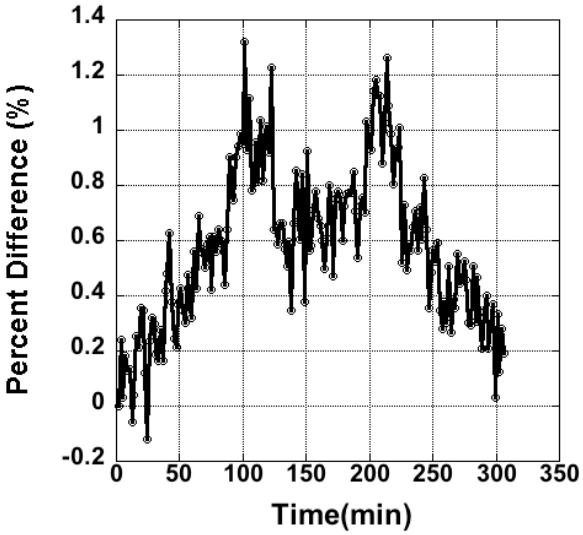

Fig. 3. Variation of the photopeak positions of the PMT coupled to NaI:Tl crystal over a period of 5 hours.

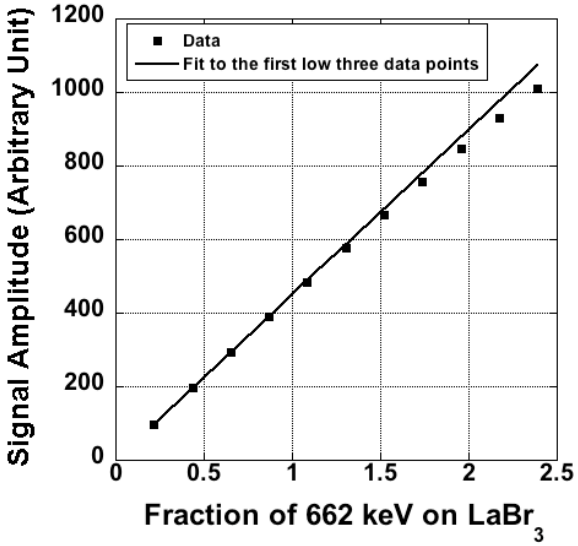

Fig. 4. Signal amplitude of the PMT versus light pulser power (calibrated as fraction of the light-yield from a $LaBr_3$ crystal when excited with 662 keV).

separate conversion factor for every ten-minute segment of the run, which is then used to calibrate the coincidence data.

C. PMT Stability

The stability of the PMT signal is also important, as variations in the PMT gain are indistinguishable from deviations from the scintillator proportionality. Therefore, the photopeak position of the PMT coupled to a scintillator sample was monitored in ten-minute segments over a period of 5 hours. The scintillator is a 1 cm diameter and 1 cm high cylindrical NaI:Tl crystal. Fig. 3 shows the variation of the photopeak positions over the whole duration. The statistical accuracy for each measurement is 0.02% and there is about a 1.2% maximum variation in the photopeak position during the 5-hour period, which is typical of gain drift in a PMT. Like the HPGe3 detector, these variations are removed via the calibration, as the singles events are used to create a separate PMT conversion factor for each ten-minute segment of the run.

D. PMT Linearity

The response of the PMT is characterized using a light pulser. The design of the light pulser is based on a variant of the method described in [9], which has the advantage of characterizing the response of the PMT over a large dynamic range. The light pulse is generated using light-emitting diodes (LEDs), Vishay model TLWB7600, which have an emission wavelength of 460 nm and a pulse width of 20 ns FWHM. The light intensity is adjusted over a 11:1 dynamic range with an accuracy of 0.1% and is calibrated as a fraction of the light yield of a $LaBr_3$ crystal coupled to the PMT when excited with 662 keV emissions of a Cs-137 source.

Since most linear focused PMTs have excellent proportionality for moderate anode currents, we fit a straight line through the first three data points. Fig. 4 shows the signal amplitude of the PMT as a function of the light pulser intensity. The PMT starts to deviate from linearity when the light pulse is close to the light-yield of a 662 keV gamma-ray on a $LaBr_3$ crystal. For crystals with light-yield comparable to or less than the light-yield of $LaBr_3$, the PMT exhibit excellent linearity. We estimate that the maximum deviation from linearity to be less than 0.5% for the range of applicable light yield.

E. Analysis and Light Yield Non-Proportionality

Since NaI:Tl is the most frequently studied inorganic scintillator and its electron response has been characterized extensively [7, 10-12], it was chosen to benchmark SLYNCI. Two samples of NaI:Tl (both 1 cm diameter, 1 cm high cylindrical crystals) are used in the non-proportionality measurements.

A total of 1,500,000 coincidence events are acquired for each of the two source-collimator positions. Only events where exactly two detectors triggered (the PMT and any one of the HPGe detectors) are used in the analysis, which is about 91% of the acquired coincidence events. For each event, the electron energy deposited in the scintillator (E_e) is deduced from the energy deposited in the HPGe detector (E_{HPGe}) using conservation of energy:

$$E_e = 661.657 - E_{HPGe} \quad , \quad [\text{keV}] \qquad (1)$$

where 661.657 is the energy of the gamma-ray emission from Cs-137 in keV [13]. Furthermore, the light yield is defined as the amplitude of the signal detected by the PMT calibrated such that the photopeak of the gamma-rays from a Cs-137 source is at 661.657.

Fig. 5 and 6 show the scatter plots of the light yield versus the electron energy deposit of one NaI:Tl sample for the two source-collimator positions (0° and 15° respectively). These plots show the valid Compton coincidence events (events where the gamma-ray from the source undergoes a Compton interaction in the scintillator and the scattered gamma-ray deposit all its energy in the HPGe detector) occupying a region along a diagonal band going through the origin as required by the conservation of energy.

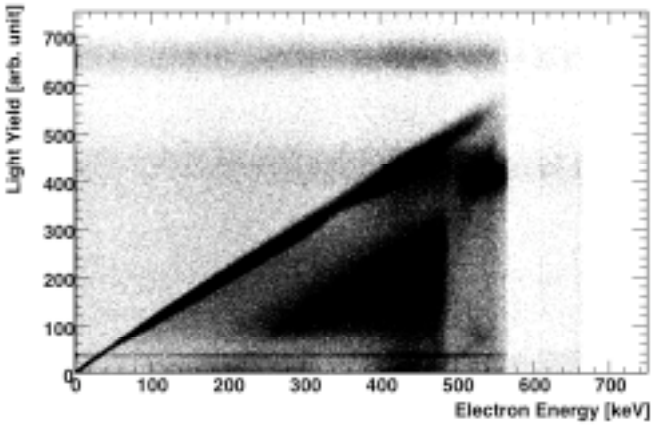

Fig. 5. Light yield versus electron energy of NaI:Tl for source-collimator position at 0°.

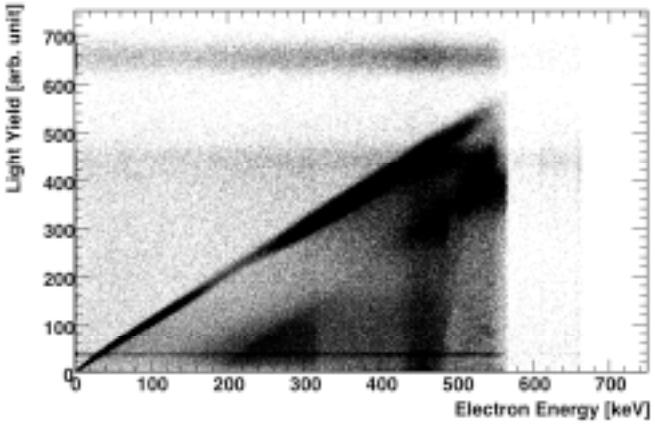

Fig. 6. Light yield versus electron energy of NaI:Tl for source-collimator position at 15°.

In addition to the valid Compton coincidence events, there are several sources of background visible in Fig. 5 and 6. First, the scattered gamma-ray can deposit a fraction of its energy in the HPGe detector by undergoing a Compton interaction in the HPGe detector followed by the scattered gamma-ray escaping the HPGe detector. Using Eq. (1), these events would be assigned an electron energy deposited in the scintillator that is higher than the correct value. Thus, these events populate the large region below the diagonal band of valid events and are well separated from the Compton coincidence events.

Second, the incident gamma-ray can undergo multiple Compton interactions before the scattered gamma-ray exits the scintillator. These events can deposit more energy than the maximum energy deposited from a single Compton interaction, which is 477 keV for a 662 keV source. The electron energy calculated from the energy deposited in the HPGe detector is also higher than the correct value because the scattered gamma-ray energy from multiple Compton interaction is lower. According to Monte Carlo simulation, these events can populate the region along the diagonal band going above 477 keV in electron energies. The fractions of events with single Compton interaction and multiple Compton interactions in a 1 cm diameter and 1 cm high cylindrical NaI:Tl crystal are 68.1% and 7.5% respectively.

Finally, the random coincidence events populate almost the

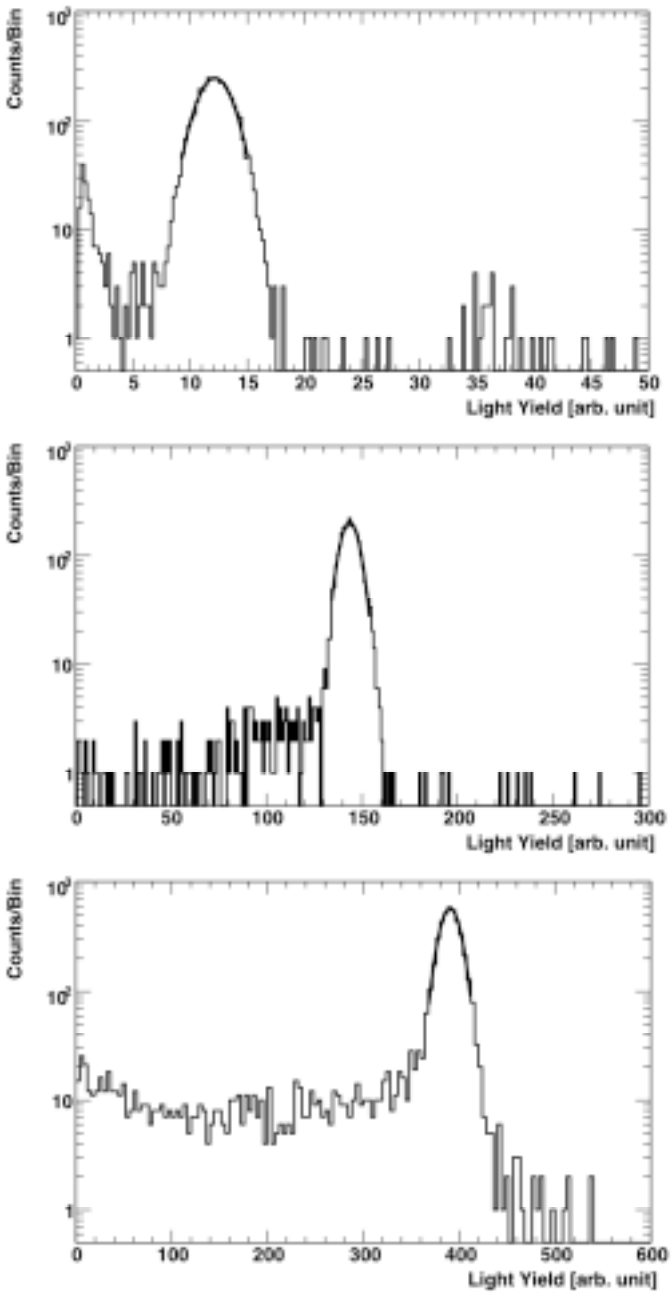

Fig. 7. Pulse height spectra of the light yield for E_e=10.5 keV (top panel), 139 keV (middle panel), and 398 keV (bottom panel).

entire scatter plot. The singles event rate is about 2000 cps for both the PMT and the OR of the five HPGe detectors, and the width of the coincidence time window is 1 μs. Thus, the random coincidence rate is about 8 cps, which is 15% of the coincidence rate. However, the random events do not pose any problem in the analysis because few random events actually populate the diagonal band in the scatter plots. By assuming that the random events populate the scatter plots in Fig. 5 and 6 uniformly, we estimate that less than 2% of the random coincidence events are inside the diagonal band. This low level of random events inside the diagonal band is further illustrated in Fig. 7, which shows the projections along the light yield axis for different vertical slices (the width of the energy window slices range from 0.5 keV for low electron

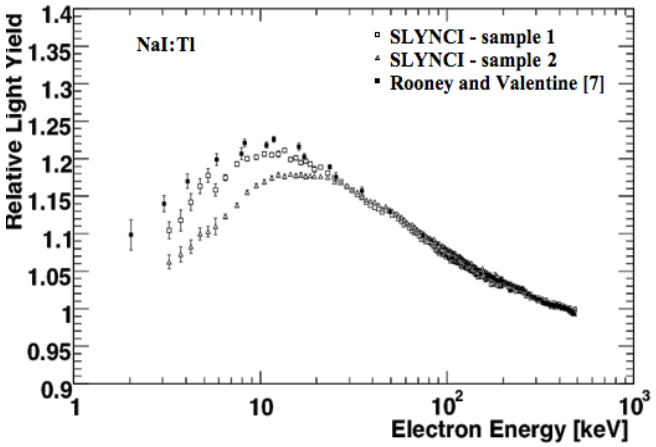

Fig. 8. Light yield response as a function of electron energy for NaI(Tl). Data are arbitrarily normalized to each other at 444 keV.

energies to 4 keV for high electron energies) of the electron energy deposited in Fig. 5 or 6. In Fig. 7, the peaks correspond to the Compton coincidence events (i.e., those on the diagonal band). The events to the left of the peaks are caused both by random events and events where the scattered gamma ray underwent a Compton interaction in the HPGe detector and escaped. Events to the right of the peaks correspond only to random events, and it is clear that the occupancy of the random events is over two orders of magnitude lower than the maximum of the peak. However, the random events are not uniformly distributed over the scatter plots, but do have a few prominent features: (1) the NaI:Tl photopeak from the gamma-rays emissions of the Cs-137 source appears as a horizontal band of events around 662 on the light yield axis; (2) the NaI:Tl Compton events populate the region above the diagonal band but below the NaI:Tl photopeak events (the Compton edge clearly visible); and (3) the fluorescent x-rays from the Cs-137 source interacting in the scintillator appear as a narrow horizontal band of events around 40 on the light yield axis. However, this structure does not affect the conclusion that random backgrounds are negligible.

In the analysis, the light yield of the events that fall within an energy slice of a specific electron energy deposited is histogrammed. Fig 7 shows the histograms for three different electron energy deposits (E_e=10.5, 139, and 398 keV). Each histogram is required to have a minimum of 1000 events. The width of the energy slice depends on the electron energy, ranging from 0.5 keV (for the low electron energy events) to 4 keV (for the high electron energy events). The centroid of the peak, which represents the average light yield for the electron energy in the scintillator, L, is determined by fitting the peak with a Gaussian function. Assuming the electron energy distribution in each energy slice is uniform, the average electron energy is taken to be the mid-point within the energy slice. The relative light yield per electron energy is calculated by the ratio L / E_e.

Fig. 8 shows the electron response of two NaI:Tl crystals measured with SLYNCI. The results are compared with the measurement made with the original Compton coincidence instrument by Rooney and Valentine [7]. The data are normalized at 444 keV, the highest electron energy reached by the data from Rooney and Valentine. Note that the Rooney and Valentine data consist of 20 electron energy values and took about a month to measure, while the SLYNCI data consist of 180 electron energy values and took one day to measure. All the data agree reasonably well above 30 keV. While the data start to deviate from each other below 30 keV, the general trend remains the same (i.e., the relative light yield peaks around 10 keV). The stability of the SLYNCI measurement is tested by repeating the measurement at different times and also by recoupling the crystal to the PMT. The same results are obtained to within statistical error for each sample. The deviation in the data below 30 keV may be attributed to the sample-to-sample variation. Although the SLYNCI is designed to sample the electron energy down to 1 keV, there are some difficulties in analyzing the data below 3 keV because of the noise level of the PMT, which requires a higher threshold setting in reading out the PMT signal. In addition, accurate calibration of the HPGe is very important because the analysis is very sensitive to small differences in the electron energy deposit calculations for low electron energies as discussed in Section IV.

IV. Systematic Effects

We study several potential sources of systematic error using data from a Monte Carlo simulation. The SLYNCI events are simulated using the GEANT4 simulation package [14-15], where the simulation includes energy and material dependent Compton interactions, photoelectric interactions, fluorescent x-ray creation, and Auger electron production in the collimator, scintillator crystal, and HPGe detectors.

We evaluate potential sources of systematic error by introducing an error into the simulation, computing the "measured" electron response, and comparing the result to the "true" electron response that was input to the simulation. The most sensitive source of error is found to be the HPGe detector calibration. An incorrect multiplicative factor was assumed, given by $E_{meas} = E_{true} \cdot (1+\delta)$, where E_{meas} was the "measured" energy in the HPGe detector, E_{true} was the true energy deposited in the HPGe detector, and δ is the error. The data are shown in Fig. 9 for several different values of the incorrect calibration constant, as well as the true calibration. The conclusion is that the measurement is insensitive to HPGe calibration error for electron energies over ~20 keV, but a 0.005% error (corresponding to an energy discrepancy of ~30 eV) gives a 1% systematic effect at 2 keV electron energy. During the calibration, as discussed in Section III.A, we measure the photopeak positions of the HPGe detectors with an accuracy of 0.001%, which suggests that the electron proportionality can be measured with better than 1% accuracy over the entire electron energy range (2–466 keV).

A second source of systematic error that we explore is multiple Compton scatter in the scintillator. In this case the total amount of energy deposited in the scintillator is measured correctly, but instead of the energy being transferred to a single electron, it is divided among multiple electrons with lower energies. As the electron response depends on

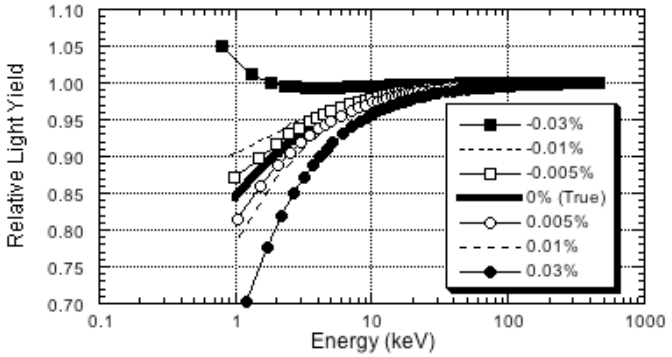

Fig. 9. Dependence of Electron Response on HPGe Energy Calibration. This figure shows how the "measured" electron response changes as a function of the error in the HPGe calibration.

electron energy, such events can give rise to systematic errors. However, the Monte Carlo simulation predicts that multiple Compton scatter in the scintillator comprises less than 10% of the "read out" events and changes the electron response by less than 1% for all electron energies.

A final source of error that we explore is Compton scatter in the source collimator, which reduces the energy of the gamma ray that impinges on the scintillator sample. Larger angle scatter is not problematic, as it produces events that fall outside the diagonal band of events in Fig. 5 and 6, but low angle scatter can reduce the energy by only a few keV and so get confused with good events. Monte Carlo simulation predicts that the rate of Compton scatter in the collimator is small (less than 1% of all "read out" events) and that it changes the electron response by less than 1% for all electron energies.

V. Future Work

Several upgrades are planned for the SLYNCI. While conventional PMTs can be designed to have excellent linearity, their gain is always prone to space-charge effects, as well as time-, temperature-, and rate-dependent gain drift. Therefore, we will replace the current PMT in the SLYNCI with a hybrid photodetector (HPD) from Photonis-DEP [16-21], which is inherently much more linear than a conventional PMT. Another important advantage of the HPD is its lower noise level and its ability to resolve single photoelectrons, which will allow the SLYNCI measurement to probe lower electron energies. In addition, we will also upgrade the current 100 MHz digitizers with 200 MHz digitizers to sample the raw waveforms more frequently. Finally, we intend to fit the digitized PMT waveform to extract the scintillation decay time as a function of electron energy. As many scintillators have multiple decay components (often corresponding to different decay mechanisms), this may provide more insight into the fundamental mechanisms of non-proportionality.

VI. Summary

A second-generation Compton coincidence facility has been constructed to study the electron response in scintillators. The performance and accuracy of the SLYNCI has been characterized by measuring the electron response of two NaI:Tl samples as a function of electron energy. The most important key feature of the SLYNCI is the increase in the event rate largely caused by eliminating the collimation that defines the deposited energy. This allows a single scintillator sample to be measured in one day, but requires that the energy calibration for the HPGe detector be extremely accurate. We have demonstrated that by interspersing the coincidence events with singles events, we can calibrate both the PMT and HPGe with sufficient accuracy that the error in the electron response is less than 1% for all measured electron energies.

Acknowledgment

This work is supported in part by the National Nuclear Security Administration, Office of Defense Nuclear Nonproliferation, Office of Nuclear Nonproliferation Research and Engineering (NA-22) of the U.S. Department of Energy under contract No. DE-AC03-76SF00098, grant number NNSA LB06-316-PD05 / NN2001000, and in part under the auspices of the U.S. Department of Energy by University of California, Lawrence Livermore National Laboratory under Contract W-7405-Eng-48, and by the Domestic Nuclear Detection Office of the Department of Homeland Security.

References

[1] J. D. Valentine and B. D. Rooney, "Design of a Compton spectrometer experiment for studying non-linearity and instrinsic energy resolution," *Nucl. Instr. Meth.*, A353, pp. 37-40, 1994.

[2] P. Dorenbos, J. T. M. de Haas, and C. W. E. van Eijk, "Non-proportionality in the scintillation response and the energy resolution obtainable with the scintillation crystals," *IEEE Trans. Nucl. Sci.*, vol. 42, pp. 2190-2202, 1995.

[3] J. D. Valentine, B. D. Rooney, and J. Li, "The light yield nonproportionality component of scintillator energy resolution," *IEEE Trans Nucl. Sci.*, vol. 45, pp. 512-517, 1998.

[4] E. V. D van Loef, W. Mengesha, J. D. Valentine, P. Dorenbos, and C. W. E. van Eijk, "Nonproportionality and energy resolution of a $LaCl_3$:10% Ce^{3+} scintillation crystal," *IEEE Trans Nucl. Sci.*, vol. 50, pp. 155-158, 2003.

[5] M. Balcerzyk, M. Moszynski, M. Kapusta, D. Wolski, J. Pawelke, *et al.*, "YSO, LSO, GSO and LGSO. A study of energy resolution and nonproportionality," *IEEE Trans Nucl. Sci.*, vol. 47, pp. 1319-1323, 2000.

[6] M. Moszynski, J. Zalipska. M. Balcerzyk, M. Kapusta, W. Mengesha, *et al.*, "Intrinsic energy resolution of NaI(Tl)," *Nucl. Instr. Meth.*, A484, pp. 259-269, 2002.
[7] B. D. Rooney and J. D. Valentine, "Benchmarking the Compton coincidence technique for measuring electron response non-proportionality in inorganic scintillators," *IEEE Trans. Nucl. Sci.*, vol. 43, pp. 1271-1276, 1996.
[8] W.-S. Choong, K. M. Vetter, W. W. Moses, G. Hull, S. A. Payne, N. J. Cherepy, and J. D. Valentine, "Design of a facility for measuring scintillator non-proportionality," accepted for publication in *IEEE Trans. Nucl. Sci*., 2008.
[9] M. Vicic, L. G. Sobotka, J. F. Williamson, R. J. Charity, and J. M. Elson, "Fast pulsed UV light source and calibration of non-linear photomultiplier response," *Nucl. Instr. Meth.*, A507, pp. 636-642, 2003.
[10] C. D. Zerby, A. Meyer, and R. B. Murray, "Intrinsic line broadening in NaI(Tl) gamma-ray spectrometers," *Nucl. Instr. Meth.*, 12, pp. 115-123, 1961.
[11] F. T. Porter, M. S. Freedman, F. Wagner, Jr. and I. S. Sherman, "Response of NaI, Anthracene and plastic scintillators to electrons and the problems of detecting low energy electrons with scintillators counters," *Nucl. Instr. Meth.* 39, pp. 35-44, 1966.
[12] R. Hill and A. J. L. Collinson, "The effect on the scintillation efficiency of NaI(Tl) of changes in the thallium concentration and strain," *Brit. J. Appl. Phys.*, vol. 17, pp. 1377-1383, 1966.
[13] L. P. Ekstrom and R. B. Firestone, WWW Table of Radioactive Isotopes, database version 2/28/99 from URL http://ie.lbl.gov/toi/index.htm.
[14] S. Agostinelli, J. Allison, K. Amako, J. Apostolakis, H. Araujo, P. Arce, *et al.*, "GEANT4–a simulation toolkit," *Nucl. Instr. Meth.*, A506, pp. 250-303, 2003.
[15] J. Allison, K. Amako, J. Apostolakis, H. Araujo, P. Arce Dubois, M. Asai, *et al.*, "Geant4 developments and applications," *IEEE Trans. Nucl. Sci.*, 53, pp. 270-278, 2006.
[16] R. DeSalvo, "Why people like the hybrid photodiode," *Nucl. Instr. Meth.*, A387, pp. 92-96, 1997.
[17] C. P. Datema, "Hybrid photodiodes in scintillation counter applications," *Nucl. Instr. Meth.*, A387, pp. 100-103, 1997.
[18] C. D'Ambrosio, C. Ercoli, S. Jaaskelainen, G. Lecoeur, H. Leutz, *et al.*, "A HPMT based set-up to characterize scintillating crystals," *Nucl. Instr. Meth.*, A434, pp. 387-398, 1999.
[19] F. De Notaristefani, F. Vittori, and D. Puertolas, "A new hybrid photomultiplier tubes as detector for scintillating crystals," *Nucl. Instr. Meth.*, A480, pp. 423-430, 2002.
[20] C. D'Ambrosio and H. Leutz, "Hybrid photon detectors," *Nucl. Instr. Meth.*, A501, pp. 463-498, 2003.
[21] M. Moszynski, W. Klamra, D. Wolski, W. Czarnacki, M. Kapusta, *et al.*, "Comparative study of PP0275C hybrid photodetector and XP2020Q photomultiplier in scintillation detector," *J. Inst.*, vol. 1, pp. 1-10, 2006.